Upper critical fields in a $FeSe_{0.5}Te_{0.5}$ superconducting single crystal

D. Velasco- Soto, F.J Rivera-Gómez, C.R. Santillán-Rodríguez, R.J. Sáenz-Hernández, M.E. Botello-Zubiate, and J.A. Matutes-Aquino

Abstract

A single crystal with a nominal composition $FeSe_{0.5}Te_{0.5}$ was obtained by the Bridgman method. A quartz ampulla with the sample inside was vacuum-sealed and maintained at 1050 °C for 37 h to homogenize the sample. Subsequently, the quartz ampulla with the sample was moved with a speed of 2.2 mm/h to a furnace which was at 450 °C. X-ray diffraction confirmed the tetragonal structure of the grown single crystal with the cleavage plane corresponding to the ab plane. Resistance measurements were carried out with magnetic fields from 0 to 9 T, applied parallel to the c axis and ab plane, respectively. A zero-field critical temperature T_c=14K was determined. The upper critical field vs. temperature phase diagram was built for temperatures where the resistance drops to 90%, 50%, and 10% of the normal state resistance. The linear extrapolation to T=0K gave upper critical fields of 57.2, 51.8, and 46.0 T for H||c axis and 109.6, 95.5, and 80.9 T for Hjjab. Applying the Werthamer–Helfand–Hohenberg (WHH) theory, upper critical fields of 39.6, 35.9, and 31.8 T and coherence lengths of 28.8, 30.3, and 32.1Å were obtained for Hjjc; while for Hjjab, upper critical fields of 51.3, 40.7, and 37.5 T and coherence lengths of 22.3, 26.7, and 31.5Å were obtained. The value of μ_0H_{c2}/k_BT_c calculated by the WHH theory exceeds the Pauli limit (1.84 T/K) indicating the unconventional nature of superconductivity. The activation energy U0 has two different rates of change with the applied magnetic field probably due to two different

thermal activation mechanisms; the origin of which requires further investigation. A similar behavior is observed in the irreversibility lines.

Introduction

The discovery of the new families of iron-based superconductors, starting with the discovery of superconductivity in La $[O_{1-x}F_x]FeAs$ compounds, opened new routes in the investigation of high temperature superconductivity mechanisms.[1] At least, five families of iron-based superconductors have been discovered.[2,3] The $FeSe_xTe_{1-x}$ system has been studied since the discovery of superconductivity in FeSe by Hsu *et al*. in 2008.[4]

This work presents a magneto-transport study of a tetragonal $FeSe_{0.5}Te_{0.5}$ single crystal grown by the Bridgman method. Upper critical fields, coherence lengths, thermal activation energies, and irreversibility lines were determined.

Experimental methodology

A single crystal with tetragonal structure and nominal composition $FeSe_{0.5}Te_{0.5}$ was grown by the Bridgman method encapsulating the material in a vacuum-sealed double wall quartz ampoule. The sample was prepared from selenium and tellurium powder and iron chunks. First, the sample was melted and homogenized at 1050 °C during 36 h. Then, the sample was moved through the temperature gradient formed between two ovens with temperatures of 1050 °C and 450 °C, respectively, at a rate of 2.2 mm/h.

Magnetotransport measurements were made by the four-point method with the applied magnetic fields parallel to the c axis and also parallel to the (001) or ab plane using a Quantum Design Physical Property Measurement System.

Results and discussion

The X-ray diffraction pattern of a sheet of material cleaved from the original single crystal showed only reflections from the (001) plane indicating that the sample surface is perpendicular to the c crystallographic axis. Fig. 1 shows resistivity (normalized to the normal state value) versus temperature for applied magnetic fields of 0, 1, 2, 3, 4, 5, 6, 7, 8, and 9 T, (a) H||c and (b) H||ab. In both cases, the electric current was applied parallel to the ab plane. The width of the zero-field resistive superconducting transition is approximately 1.3 K.

From these data, the H-T phase diagram (Hc2 critical field versus temperature) shown in Fig. 2 was constructed, where the empty and full symbols correspond to H||ab and H||c, respectively. For the determination of the upper critical field, H_{c2}, three criteria were used: when the resistivity falls to 90% (onset), 50% (mid), and 10% (offset) of its normal state value. Under these criteria, critical temperatures of 14.6, 14.0, and 13.2 K, respectively, were determined at 0 T. Then the critical fields $_{\mu0}H_{c2}$ at 0K were determined first by extrapolating the H_{c2} lines versus T to 0K and second by calculating the slope of the H-T phase diagram at T_c and using the WHH (Helfand-Hohenberg-Werthamer) theory formula.[2,5–7]

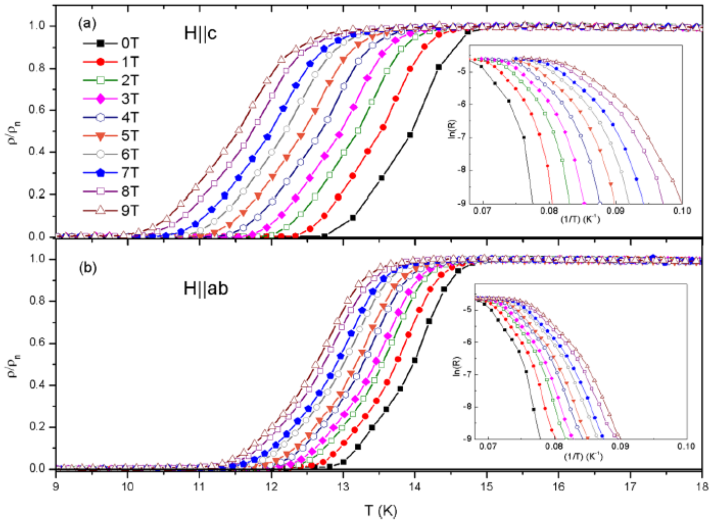

FIG. 1. Resistivity (normalized to the normal state resistivity) versus temperature for magnetic applied magnetic fields of 0, 1, 2,3,4,5,6,7,8, and 9 T, (a) H||ab and (b) H||c. Insets: Arrhenius plots for the same applied magnetic fields (a) H||ab and (b) H||c.

$$\mu_0 H_{c2}(0) = -0.693\mu_0 (dH_{c2}/dT)_{T_C} T_C. \qquad (1)$$

Coherence lengths in the ab plane, ξ_{ab}, and along the c axis, ξc, were estimated at 0K from the formulas of the Ginzburg-Landau theory,

$$\xi_{ab} = (\Phi_0/2\pi\mu_0 H_{c2}^{\|c})^{1/2}, \quad \xi_c = \Phi_0/2\pi\xi_{ab}\mu_0 H_{c2}^{\|ab}, \qquad (2)$$

where Φ_0 is the magnetic flux quantum, μ_0 is the magnetic $H_{c2}^{\|c}$ and $H_{c2}^{\|ab}$ are the critical fields parallel to the c axis and ab plane, respectively, at T=0 K. The calculated values of $\mu_0 H_{c2}/k_B T_c$, using H_{c2} obtained from the WHH theory, exceed the Pauli limit (1.84 T/K), which indicates the unconventional nature of superconductivity in this material. All these results are listed in Table I.

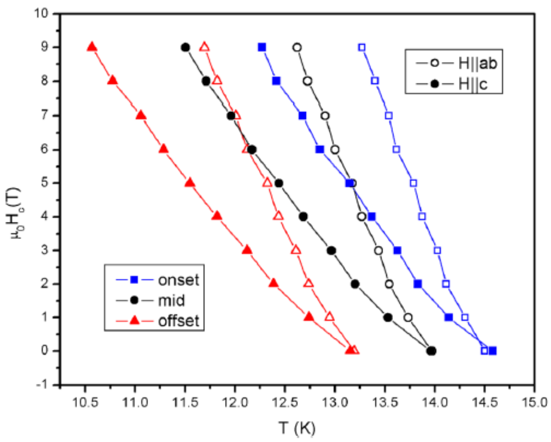

FIG. 2. H_{c2} critical field versus temperature (H-T phase diagrams) determined for conditions $R = 0.9R_n$, (onset), $R = 0.5R_n$, (mid) and $R = 0.1R_n$, (offset) where R_n is the normal state resistance. Full and empty symbols correspond to H||c and H||ab, respectively.

The vortex dynamics in a sample can be inferred based on the behavior of resistance as a function of temperature, and an Arrhenius-type behavior indicates the existence of a thermally assisted flux flow (TAFF) regimen.[9] The linear region of each curve showed in the insets of Fig. 1 follows the Arrhenius equation $\rho(T,H) = \rho_0\exp[-U_0(H)/K_BT]$, where $U_0(T)$ is the activation energy5,10–13 for the movement of vortices pinned to defects in the sample. From the slopes of these curves, the value of $U_0(t)/k_B$ for each magnetic field is obtained, and the Fig. 3(a) shows $U_0(t)/k_B$ as a function of the applied magnetic field. This function obeys the relationship U_0 α $H^{-\alpha}$.5 For H||c, α=0.07 in the range 1 T <H<5 T while α=0.85 in the range 5 T < H<9 T. The activation energy varies between 1011K and 524 K. On the other hand, for H||ab, α=0.09 in the range 1 <(H< 3T and α= 0.31 in the range 3 T <H<9 T. In this case, the activation energy varies between 607K and 398 K. The discontinuity in the slope of the curves of activation energy as a function of the magnetic field requires further study, and it could be associated with two different activation mechanisms above and below the crossover.[14]

In Fig. 3(b), a discontinuity is also observed in the slope of the irreversible field as function of temperature. The irreversibility line was determined from the curves of normalized electrical resistance as a function of temperature, calculating the points at which the resistivity drops to 10% corresponding to the normal state. To understand why in Fig. 3(b) the irreversibility line for Hkab is above the irreversibility line for Hkc, while the activation energy curve for Hkc is above the activation energy curve for Hkab, it is important to consider that the sample is highly anisotropic, has a large penetration length[15,16] and small coherence lengths, with ξ_c lower than ξ_{ab} (see Table I), and that these three properties decrease the pinning energy but at the same time tend to increase the pinning force.[9]

TABLE I. $d(\mu_0 H)/dT$, critical fields (extrapolating at $T = 0$ K and from WHH theory), coherence length, and $(\mu_0 H_{c2})/(k_B T_c)$ for magnetic fields parallel to the c axis to the ab plane.

Magnetic field direction	Criterion	$d(\mu_0 H)/dT$ (T/K)	$\mu_0 H_{c2}$ (extrapolation) (T)	$\mu_0 H_{c2}$ (WHH theory) (T)	$\xi(0)$ (Å)	$(\mu_0 H_{c2})/(k_B T_c)$ (T/K)
H‖c	Onset	−3.96	57.2	39.6	28.8	2.72
	Mid	−3.75	51.8	35.9	30.2	2.57
	Offset	−3.53	46.0	31.8	32.1	2.42
H‖ab	Onset	−7.59	109.6	51.3	22.3	3.54
	Mid	−6.87	95.5	40.7	26.7	2.93
	Offset	−6.17	80.9	37.5	31.5	2.84

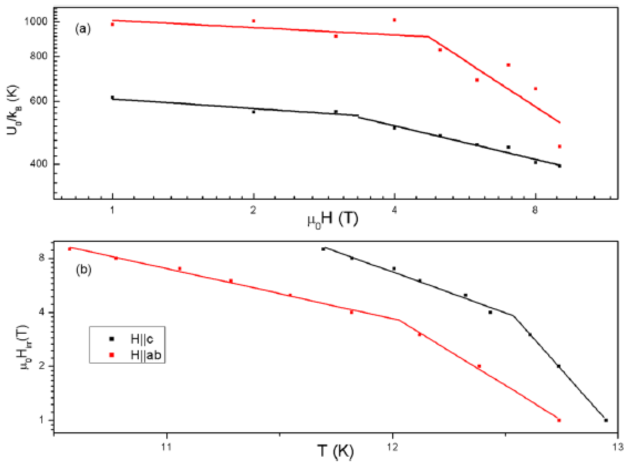

FIG. 3. (a) Activation energy versus applied magnetic field, in the H||ab and H||c directions, respectively. (b) Irreversibility line $\mu_0 H_{irr}$ versus temperature in the H||ab and H||c directions, respectively.

Conclusions

Resistance measurements with fields applied parallel to the c axis and ab plane together with the H-T phase diagram show that the grown $FeSe_{0.5}Te_{0.5}$ single crystal is highly anisotropic. Critical upper fields calculated by data extrapolation are higher than that calculated from the WHH theory. Coherence lengths, ξ_{ab}, with fields applied parallel to the c axis are greater than ξc with fields applied parallel to the ab plane. Calculated value of $\mu 0H_{c2}/k_BT_c$ using the WHH theory exceeds the Pauli limit (1.84 T/K), which indicates the unconventional nature of superconductivity in the sample. In the low resistive region of the superconducting transition, a thermally assisted flux flow behavior was observed indicating two different thermal activation mechanisms; the origin of which requires further investigation. A similar behavior is observed in the irreversibility lines.

Acknowledgments

Authors would like to acknowledge CONACYT Project No. 105865 for financial support.

References

1 Y. Kamihara, H. Hiramatsu, M. Hirano, R. Kawamura, H. Yanagi, T. Kamiya, and H. Hosono, J. Am. Chem. Soc. 128, 10012 (2006).

2 H. Lei, R. Hu, E. S. Choi, J. B. Warren, and C. Petrovic, Phys. Rev. B 81, 094518 (2010).

3 D. C. Johnston, Adv. Phys. 59, 803–1061 (2010).

4 F. C. Hsu, J. Y. Luo, K. W. Yeh, T. K. Chen, T. W. Huang, P. M. Wu, Y. C. Lee, Y. L. Huang, Y. Y. Chu, D. C. Yan, and M. K. Wu, Proc. Natl. Acad. Sci. U.S.A. 105, 14262 (2008).

5 C. S. Yadav and P. L. Paulose, New J. Phys. 11, 103046 (2009). 6J. Ge, S. Cao, S. Shen, S. Yuan, B. Kang, and J. Zhang, Solid State Commun. 150, 1641 (2010).

7 T. Ki da, T. Matsunaga, M. Hagiwara, Y. Mizuguchi, Y. Takano, and K. Kindo, J. Phys. Soc. Jpn. 78, 113701 (2009).

8 M. Tinkham, Introduction to Superconductivity (McGraw-Hill, New York, 1996).

9 E. H. Brandt, Rep. Prog. Phys. 58, 1465 (1995).

10 T. T. M. Palstra, B. Batlogg, L. F. Schneemeyer, and J. V. Waszczak, Phys. Rev. Lett. 61, 1662 (1988).

11 Y. Z. Zhang, Z. A. Ren, and Z. X. Zhao, Supercond. Sci. Technol. 22, 065012 (2009).

12 Y. Z. Zhang, Z. Wang, X. F. Lu, H. H. Wen, J. F. de Marneffe, R. Deltour, A. G. M. Jansen, and P. Wyder, Phys. Rev. B 71, 052502 (2005).

13 X. L. Wang, S. R. Ghorbani, S. X. Dou, X. L. Shen, W. Yi, Z. C. Li, and Z. A. Ren, preprint arXiv:0806.1318 (2008).

14 C. Attanasio, M. Salvato, R. Ciancio, M. Gombos, S. Pace, S. Uthayakumar, and A. Vecchione, Physica C 411, 126 (2004).

15 M. Bendele, S. Weyeneth, R. Puzniak, A. Maisuradze, E. Pomjakushina, K. Conder, V. Pomjakushin, H. Luetkens, S. Katrych, A. Wisniewski, R. Khasanov, and H. Keller, Phys. Rev. B 81, 224520 (2010).

16 T. Klein, D. Braithwaite, A. Demuer, W. Knafo, G. Lapertot, C. Marcenat, P. Rodie`re, I. Sheikin, P. Strobel, A. Sulpice, and P. Toulemonde, Phys. Rev. B 82, 184506 (2010).